5052 *Macromolecules* **2010**, *43*, 5052–5059
DOI: 10.1021/ma1007489

Macromolecules
ARTICLE

Linear and Exponential Growth Regimes of Multilayers of Weak Polyelectrolytes in Dependence on pH

Peter Bieker and Monika Schönhoff*

Institut für Physikalische Chemie, Westfälische Wilhelms - Universität Münster, Corrensstr. 28/30, D-48147 Münster, Germany

Received April 7, 2010; Revised Manuscript Received April 27, 2010

ABSTRACT: Multilayers of poly(allyl amine hydrochloride) (PAH) and poly(acrylic acid) (PAA) are formed by layer-by-layer self-assembly at defined pH values and investigated by dissipative quartz-crystal microbalance (QCM-D) and ellipsometry. Five distinct pH regimes with different growth mechanisms and growth laws are identified. At intermediate pH values, a central regime is characterized by linear growth, accompanied by very thin and very rigid films. Adjacent regimes toward higher and lower pH show exponential layer growth, and very soft films are formed. Toward very low and very high pH, again a sharp change of mechanism occurs and the growth law becomes linear again, while very asymmetric and soft layers are formed. The symmetry of the regimes and the respective film properties are attributed to charge dilution of the polyanion or the polycation chain, respectively. In either of the five regimes the mechanism of layer formation is explained by the charge densities along the chains, as supported by ATR-FTIR experiments, and varying interchain interactions.

Introduction

Polyelectrolyte multilayers (PEM) are an interesting class of materials, and the investigation of their basic properties and the development of further applications are still growing research fields, even 20 years after their first demonstration. The layer-by-layer technique (LbL), developed by Hong and Decher,[1] is a simple and versatile technique to build up PEM. It is based on the alternating self-assembly of oppositely charged polyions onto a charged surface. The thickness of the resulting films is in the order of nanometers[2] and can be varied by adding salt to the polymer solutions.[3,4] In addition, the temperature is a factor which influences the thickness of PEM.[5] Another factor which controls the thickness of PEM is the content of water in the PEM. It has been found that a PEM contains up to 20 wt % of water in the dry state;[6] therefore, the thickness varies upon drying.[7] Various charged substances can be used for the buildup such as nanoparticles,[8] lipids,[9] proteins, and DNA by replacing one or even both polyelectrolytes with such a component. Many different polyelectrolyte structures have been used to build up PEM. The most common polyelectrolyte combinations are poly(allyl amine hydrochloride) (PAH)/poly(styrenesulfonate) (PSS) and poly(diallyldimethylammonium chloride) (PDADMAC)/(PSS).[10,11] For these films a linear growth, i.e., dependence of total layer thickness on number of layers, is observed.[12] Other combinations of polyelectrolytes can lead to an exponential growth of the PEM, which was observed for biopolymers, i.e., polypeptides and polysaccharides, for example poly(glutamic acid) (PGA)/(PAH).[13] The buildup of these exponentially growing films is accompanied by the diffusion of single chains into the film during each adsorption step, causing an adsorbed amount, which is proportional to the total layer thickness, yielding exponential growth.[14] The growth mechanism involving the diffusion of chains through the film was demonstrated by using fluorescently labeled polyelectrolyes.[15] In the paper of Elzbieciak et al. nonlinear growth of multilayers formed from the weak polyelectrolytes PAA and PAH can be seen in Figure 2 when both polyelectrolytes are not fully charged, i.e., employing pH = 3 for the PAA solution and pH = 11 for the PAH solution, though the authors do not point this out further.[16]

Multilayers of such weak polyelectrolyte pairs, i.e., made of polyacids and polybases, are interesting since the degree of charge of the chains and thus the film properties can be controlled by the pH of the polymer solution. The most common weak polyelectrolyte pair employed in PEM formation is poly(acrylic acid) (PAA)/(PAH). By ellipsometric studies of a dried layer pair of PAA/PAH, Shiratori and Rubner found a thickness of the layer pair that depended on the pH value of the polyelectrolyte solutions.[17,18] They identified the charge density on the adsorbing chain and the surface charge density of the last adsorbed layer as the main parameters controlling the layer thickness.

It was further shown that the pK_a value of a weak polyelectrolyte changes when it is incorporated in PEM.[19,20] For example, the pK_a value of PAA shifts to smaller values upon incorporation of PAA into PEM, since the complexation to polycation charges favors the dissociated form of the polyacid.[20] Similarly, a shift of the pK_a value of polybases has been reported, and this shift was larger when the pH value of the polyelectrolyte solution was different from the pK_a value.[19] The shift was largest for the first layer and was less pronounced with each additional layer of PAA and PAH in the PEM. Salt ions did not have an influence on the pK_a value.[21] Charging and discharging of internal groups by pH variation has been employed in controlled uptake and release of single charged dyes into PEM[22] and was furthermore the basis of molecular imprinting in PEM.[23] The viscoelastic properties of PAA/PAH multilayers at a pH of 7.5 have been reported, and they were found to depend strongly on the type of outermost layer.[24]

Very recently, Fujii et al.[25] studied the pH-dependent multilayer formation for a weak polyelectrolyte pair with a large charge-to-mass ratio. They report on the dependence of layer thickness and roughness on pH. All of the papers studying

*Corresponding author: Ph +49-251-8323419, Fax +49-251-29138, e-mail schoenho@uni-muenster.de.

 Published on Web 05/07/2010

pH-dependent layer formation agree in finding low thickness values for strongly charged chains and an enhanced thickness for weakly charged chains. However, no analysis of the growth laws of PEM formation employing weak polyelectrolyte pairs has been reported so far.

Here, we investigate the buildup of PAA/PAH in the pH region from pH 3 to pH 11 by QCM-D and ellipsometry. By analyzing the data by the Kelvin−Voigt model and fitting the adsorption curves of the QCM data, we are able to characterize the growth behavior of the films. We find that with increasing pH of the polymer solutions the layer formation shifts from a linear to an exponential growth behavior and back. Regimes with different growth laws, which are sharply separated, are centered around the neutral pH region. The total thickness is independent of the growth behavior of the films. We can relate both the type of growth law and the thickness to the degree of charge of either polyelectrolyte component and clarify the mechanisms of layer formation in either growth regime.

Materials and Methods

Polyelectrolytes. Branched poly(ethylenimine) (PEI) (M_w = 50 000−60 000), poly(acrylic acid) (PAA) (M_w = 100 000), and poly(allylamine hydrochloride) (PAH) ($M_w \sim 56\,000$) have been purchased from Sigma-Aldrich. The concentration of all polyelectrolyte solutions is 0.01 mol/L with respect to the monomer unit. Each solution, including washing solution, is adjusted to a fixed pH value by addition of either 0.1 mol/L NaOH or 0.1 mol/L HCl, both purchased from Honeywell. The maximum concentration of sodium or chloride ions, which arises due to the adjustment of the pH value, is 0.07 mol/L. Water employed for all solutions and rinsing processes is ultrapure water (ρ > 18 MΩ·cm) purified in a Milli-Q Academic purification stage (Millipore).

Quartz Crystal Microbalance (QCM). The buildup of the PEM was monitored in situ by a quartz crystal microbalance using a flow chamber (QCM-D, E4, QSense, Götenborg, Sweden). For all measurements quartz crystals with a gold coated surface and a fundamental frequency of 5 MHz, purchased from QSense, are used. Prior to use, the quartz crystals are cleaned with RCA solution, which is a mixture of 25% ammonia solution (Acros), 35% hydrogen peroxide (VWR), and ultrapure water in a ratio of 1:1:5, heated for 10 min to 70 °C. All measurements are made with the crystals in flow cells where only the upper side of the crystals is in contact with the solution, and the system is under flow with a flow rate of 200 μL/min. The QCM technique consists of measuring the change of the resonance frequency of a quartz crystal (Δf), which is induced by polyelectrolyte adsorption onto the crystal. The reference frequency is given by the resonance frequency of the crystal in contact to ultrapure water. For the PEM buildup the polyelectrolyte solution is rinsed over the crystal for 15 min, followed by washing for 5 min. All solutions employed in one multilayer formation process are adjusted to the same pH value, even the washing solution. The first layer is always formed by PEI. The whole PEM contains 20 layers; the structure is PEI(PAA/PAH)$_9$PAA. The temperature is maintained at 20 ± 0.02 °C.

The frequency shift can be interpreted as an increase of adsorbed mass on the crystal. In addition, the dissipation of the film, which is a measure of the viscoelastic properties, is monitored. The dissipation is the reciprocal of the quality factor Q and is defined as

$$D = \frac{1}{Q} = \frac{E_{\text{dissipated}}}{2\pi E_{\text{stored}}} \quad (1)$$

where $E_{\text{dissipated}}$ is the energy dissipated during one oscillation period and E_{stored} is the energy stored during the same time interval. The dissipation for the crystal employed here is on the order of 10^{-6}. When the dissipation of the films is low, the Sauerbrey equation is valid (see eq 2).[26]

$$\Delta m = -C\Delta f \quad (2)$$

Under this condition, the relation between the frequency shift, Δf, and the added mass, Δm, is linear and C is a constant, which depends on the properties of the quartz.

For the qualitative analysis of the measurements, the plateau values of the frequency and the dissipation are determined after each washing step following the adsorption of one layer. For the determination of the total thickness of the PEM the Kelvin−Voigt model is employed. The Kelvin−Voigt model is a viscoelastic model, which describes the viscoelastic properties of the PEM with four parameters, i.e., density, viscosity, shear elasticity, and thickness.[27] In the present study, the data of the 3rd, 5th, 7th, 9th, and 11th overtones are employed in the model, and the calculations are performed by the software Q-Tools (QSense).

Ellipsometry. To determine the thickness of dry PEM, null-ellipsometry measurements are performed on a Multiskop (Optrel, Kleinmachnow) at a wavelength of 632.8 nm and at angles of incidence of 65°, 70°, and 75°. The PEM are built up on oxidized silica wafers (Silchem, oxide thickness: 300 nm). Before the adsorption of the polyelectrolytes the wafers are cleaned by the RCA method as described above. PEI(PAA/PAH)$_9$PAA multilayers are built up by immersing the substrate into polymer solution for 20 min followed by four washing steps with a washing time of 3 min each. The deposition is performed with a dipping robot DR-3 (Riegler and Kirstein, Berlin). Before measuring the thickness of a PEM, the exact thickness of the oxidized layer is measured on a noncoated area. The thickness of the PEM is obtained by using an optical model with three layers: The first layer is Si, the second is the oxidized silica with the thickness determined beforehand as a fixed parameter, and the third layer is the adsorbed PEM. On each sample, measurements at five different positions on the PEM under the three angles of incidence are performed. The deviation between these 15 measurements is less than 10 nm, and the thickness is calculated as the average of all measurements.

Attenuated Total Reflection-Fourier Transform Infrared (ATR-FTIR) Spectroscopy. ATR-FTIR measurements are performed with a twin parallel mirror setup (Harrick) in a flow cell, which is built into a FTIR spectrometer (Bruker IFS 66v/s). Adsorption of polyelectrolyte is performed on a Si crystal (Komlas GmbH), which acts as a waveguide, providing multiple total reflection. For the signal detection a liquid nitrogen-cooled MCT detector is used. Before each measurement the crystal is cleaned by RCA solution for 20 min and subsequently washed several times with ultrapure water and dried in a nitrogen gas stream. The spectrum of the Si crystal with one layer of PEI adsorbed and in contact with aqueous solution is used as a background spectrum. The adsorption time for the polymer solution is 20 min, followed by washing for 10 min. The first layer is PEI and after that one PAA layer is adsorbed.

Results

PEM Buildup Observed by QCM. Figure 1 shows the frequency change and dissipation after deposition of 20 layers of PAA and PAH observed by QCM-D. The mass coverage increment, being proportional to the negative frequency change, depends strongly on pH: While very thin multilayers are formed between pH 6 and 8, a very large layer thickness is obtained at pH = 5. The dissipation also shows large variations in dependence on pH, which do not seem directly correlated to the mass increments. Thus, multilayer buildup of the weak polyelectrolytes PAA and PAH shows different growth regimes and film properties in dependence on the pH value of the electrolyte solutions.

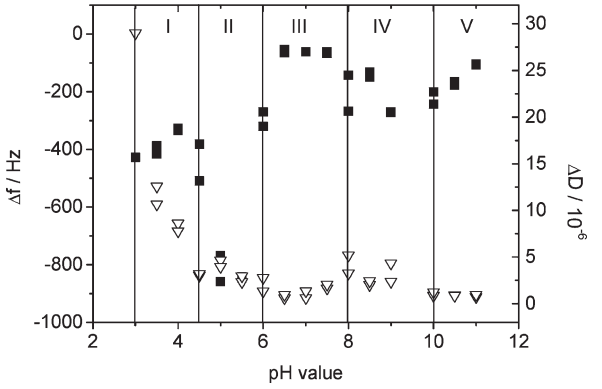

Figure 1. Frequency and dissipation increment of PEI(PAA/PAH)$_9$-PAA PEM prepared at different pH values. Filled squares: frequency change; open triangles: dissipation change.

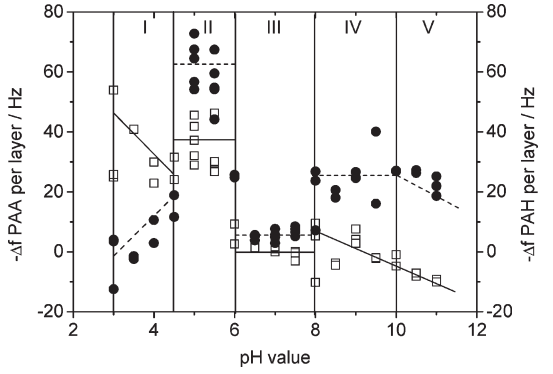

Figure 2. Average frequency change for a single layer of PAA or PAH at different pH values in a film of a total of 20 layers. Open squares: frequency change per PAA layer; filled circles: frequency change per PAH layer. Solid and broken lines are guides to the eye.

In particular, five different growth regimes can be identified as indicated in Figure 1, and they will be described here. In the first regime (regime I) from pH 3 to pH 4.5 the frequency change is large, about −400 Hz, and the dissipation values are very high, ranging from 10 to 30. Thus, in this region we obtain a rather soft and thick film. In the second region from pH 4.5 to pH 6 (regime II) the frequency change decreases dramatically to almost −900 Hz and is now more than twice the value of the frequency change in regime I. On the other hand, the dissipation decreases to values around 3. Thus, in this regime we observe less soft, but extremely thick, films. In the third region from pH 6.5 to pH 8 (regime III) the frequency change is only −70 to −100 Hz, and also the dissipation is very low, documenting the formation of a very thin, rigid film. In the fourth pH region from pH 8 to pH 10 (regime IV), the frequency shift is about −200 Hz and the dissipation slightly increases at the beginning of this regime, indicating the formation of somewhat soft films of intermediate thickness. In the fifth pH region from pH 10 to pH 12 (regime V), the frequency change is about −100 Hz and is decreasing with increasing pH. The dissipation is low with a value of 2. Thus, in this regime we obtain thin and not very soft films.

It is interesting to try to attribute these large variations in overall film thickness to the contributions of either of the two polymers. In Figure 2 the average frequency change per single layer of PAA or PAH is given for the same multilayer consisting of 20 single layers. Note that here the negative frequency shifts, $-\Delta f$, are displayed, such that large positive values correspond to large mass increments.

Again, the five regimes can be clearly identified by different frequency changes for either of the two polymers in the respective regime: In regime I the frequency change for the PAA layer is about 30 Hz per layer. In this region the PAH deposition can even decrease the frequency by up to 10 Hz, documenting a very asymmetric layer formation. In regime II both polymers reach a maximum. For PAA it is 40 Hz and for PAH 70 Hz. A different picture can be seen in the third region. Here both polymers show only a minor mass increase. In regime IV, the frequency change due to PAA adsorption is in the range of 5−0 Hz and that due to PAH adsorption is about 25 Hz. In regime V, the frequency change of the PAA is further decreased and becomes negative, similar to that for PAH in regime I. Also, the frequency change of PAH is decreased to 20 Hz per layer. Note that in the adsorbed mass per layer, the hydration water is contained. Thus, negative values of Δm (i.e., $\Delta f > 0$) indicate a loss of hydration water upon polymer adsorption, which is overcompensating the adsorbed polymer mass of this layer.

Altogether, by changing the pH value of the electrolyte solution the adsorbed mass of both polymers is strongly influenced. In regimes I and V very asymmetric layers are formed, either consisting mainly of PAH or PAA, respectively. This asymmetry is reduced in regimes II and IV, and symmetric layer growth occurs in regime III. Thus, there is a qualitative, though not quantitative, similarity in the growth behavior when increasing or decreasing the pH from the central, neutral regime III on. In how far the different adsorbed masses in each regime can be related to the degree of charge of either chain will be pointed out in the discussion.

Growth Laws of PEM. In addition to the above evaluation of overall mass increments per multilayer system and average mass increments per layer, more information about the mechanisms of layer formation can be gained by extracting the frequency changes after deposition of each single layer. Figure 3 gives the negative frequency change in dependence of the number of layers deposited. The growth law of layer buildup of PEM is extracted by a fit of the negative frequency change with the phenomenological equation

$$-\Delta f = An + B\exp(R_0 n) - 1 \qquad (3)$$

where n is the number of single layers. Here A and B represent the amplitude of a contribution with linear growth and a contribution with exponential growth, respectively. R_0 is a constant. The −1 at the end of the equation is included in order to set the offset to zero, such that it is $\Delta f(0) = 0$. Figure 3 gives two examples of such fits for multilayers prepared at different pH values. For layers prepared at pH 10 (Figure 3b), the fit function agrees well with the data points, which are slightly exponentially increasing, apart from a pronounced odd−even effect. Odd−even effects in LbL buildup have been extensively discussed in the literature;[28] in the present case, apparently upon PAA adsorption water is expelled from the film. For layers prepared at pH 5 (Figure 3a), frequency changes are generally much larger. A slightly systematic deviation of the fit from the data is observed, which is due to the increase becoming less exponential at layer numbers above 15. This will be explained further below in context with the kinetics presented in Figure 5.

In order to quantify the relative extent of exponential growth in relation to the total growth, we define a ratio

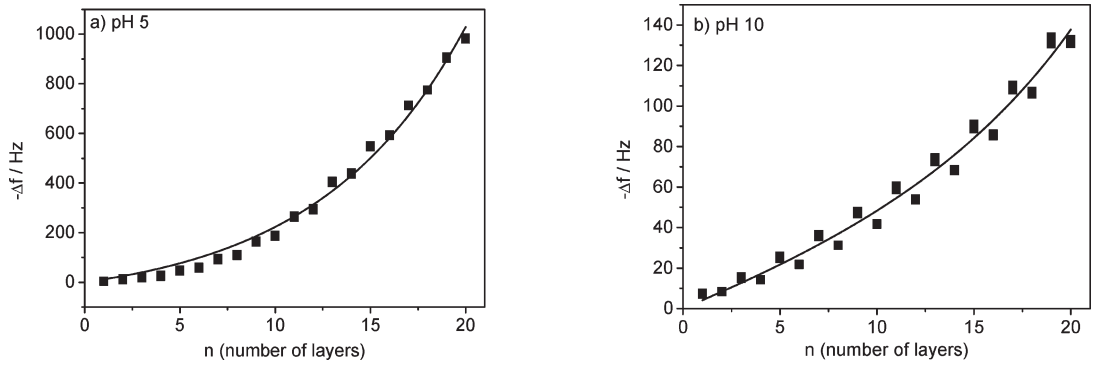

Figure 3. Negative frequency shift in dependence on the number of layers deposited, n, for PEM buildup (a) at pH = 5 and (b) at pH = 10. Data points represent experimental data, and the solid lines give the fit resulting from eq 3.

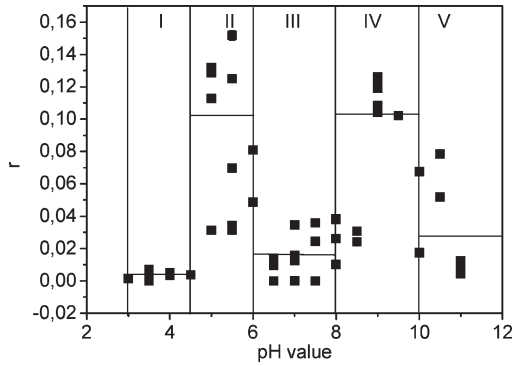

Figure 4. Results of the fit of the growth law (eq 3) displayed as the ratio r characterizing the contribution of exponential growth (eq 4) in dependence on the pH value during PEM buildup.

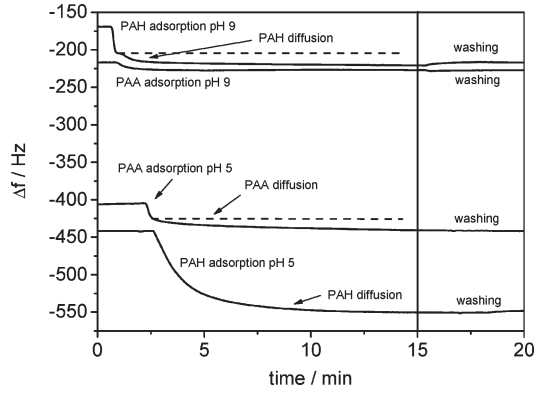

Figure 5. QCM-D raw data for the adsorption of a layer of PAA and PAH in regime IV (upper traces) and in regime II (lower traces), respectively. The horizontal, broken lines mark the end of the initial, rapid absorption. The vertical line marks the onset of the washing process.

r, which characterizes the relative relevance of exponential growth

$$r = \frac{BR_0{}^2}{A + BR_0} \tag{4}$$

The growth laws of all layer systems are fitted by eq 3, in analogy to the results shown in Figure 3. The ratio r is calculated and plotted against the pH value of the film (see Figure 4).

In Figure 4 all five growth regimes can again be identified, since they show very different degrees of exponentiality in the growth law. In the first region from pH 3 to pH 4.5 we observe an almost linear growth of the PEM, as r is nearly zero. In regime II one observes an exponential growth. Here the ratio is much larger than zero and reaches a maximum, just like both average frequency changes per layer do (see Figure 2). In regime III the growth law again is predominantly linear because the ratio is again almost zero. In the fourth region the exponentiality increases again in the same manner as the frequency is increased in Figure 1. In the last regime the ratio r decreases with further increasing pH value until a pH of 12, where no adsorption of polymers takes place. These results suggest that the differing behavior of the films concerning total thickness, single layer thickness, and dispersion in the respective regions is clearly correlated to the finding of linear or exponential growth. Evidence for exponential growth involving interdiffusion of freshly adsorbed chains into the PEM is given by a close inspection of the QCM raw data. Figure 5 shows examples for the adsorption of a PAA and PAH layer respectively in regime II (traces for pH 5) and in regime IV (traces for pH 9). Typically, an initial, rapid frequency decrease is followed by a slow frequency decrease. In the upper trace a horizontal broken line marks the end of the initial decrease of Δf. At larger times it is clearly seen that the value of Δf further decreases, i.e., the adsorbed mass increases. The initial, rapid mass increase can be attributed to adsorption of chains and the slow process to diffusion into the PEM, probably accompanied by adsorption of further chains. The same behavior is seen for PAA adsorption at pH 5. For PAA adsorption at pH 9 a second process is hard to recognize; however, this might be due to very small overall frequency changes. For PAH adsorption at pH 5 (lower trace), the interdiffusion seems to occur much faster than in the above cases, such that adsorption and diffusion processes cannot be clearly separated in time. This is probably connected with the particularly large exponentiality and layer thickness found in regime II.

An additional feature in Figure 5 explains details of the layer growth behavior in Figure 3a. It is clearly seen that the interdiffusion process is so slow that it is not finished after the adsorption time of 15 min. This is generally observed for the films in regime II, since the diffusion into thick films is very slow. For the same films, the layer growth behaves generally according to the shape shown in Figure 3a. The reduced exponential growth at layer numbers $n > \approx 15$ can thus be attributed to a limitated adsorption time. Therefore, a steady state regime of almost linear growth is established, since the layer growth is limited by the time available for diffusion.

Modeled Thickness from QCM-D Data. From the results of Figure 1 one is able to extract the thickness of the PEM by

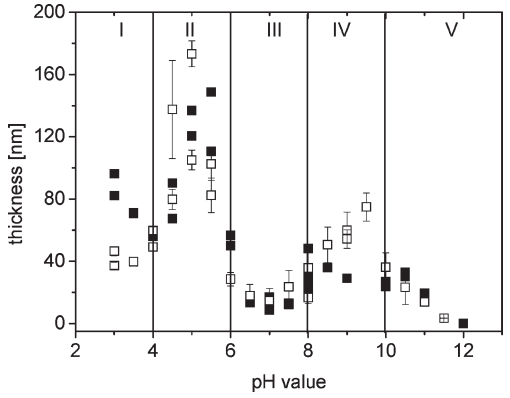

Figure 6. Film thickness of the hydrated PEI(PAA/PAH)$_9$PAA PEM calculated with the Kelvin−Voigt model from the QCM-D raw data shown in Figure 1 (filled squares) and the ellipsometric thickness of dry PEI(PAA/PAH)$_9$PAA PEM on oxidized silica wafers (open squares), both in dependence on pH during the deposition from solution. Errors of the ellipsometric data represent only the variations over one sample, whereas different data points represent different samples.

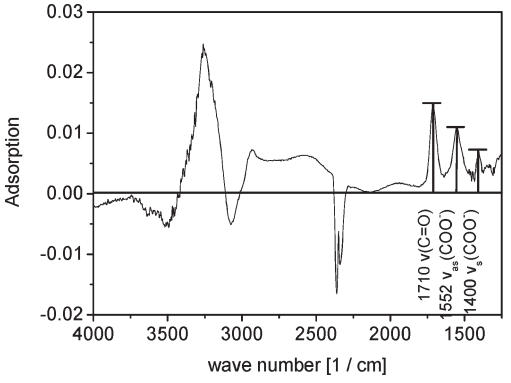

Figure 7. FTIR-ATR spectrum of a PAA monolayer adsorbed onto PEI on a silicon crystal, deposited and detected at a pH of 4 after washing.

applying a viscoelastic model to the QCM-D data. PEM are modeled as a viscoelastic solid employing the Kelvin−Voigt model. The film thickness values resulting from the modeled data are shown in Figure 6. In the first pH region an average film thickness of 60 to 90 nm is reached. This corresponds to a thickness of about 4 nm per single layer. In regime II even a total film thickness of about 130 nm is obtained, i.e., an average of 6.5 nm per single layer. These are rather large values in comparison to molecular dimensions. In regime III, however, very thin films are observed with total thickness values as low as 15 nm, which corresponds to 0.75 nm per layer. In regime IV the thickness increases again to about 40 nm, i.e., 2 nm per layer. In regime V the thickness is 30 nm and decreases with increasing pH value until a pH of 12, where no film formation is observed. These are thickness values for fully hydrated films, and in the following they are compared to the thickness of the films after drying.

Ellipsometric Measurements. The same PEM assembly consisting of 20 layers is built up on oxidized silica, and the thickness of dried layers is determined by ellipsometry. The results of these measurements are also shown in Figure 6. Again, the five regimes can be identified and show qualitatively the same behavior as the thickness values of the hydrated films. However, some pronounced differences occur between hydrated and dry layer thickness: In regime I from pH 3 to pH 4.5 the dry layer thickness is up to 40 nm smaller than the hydrated layer thickness; the discrepancy is strongly decreasing with increasing pH. This difference has to be attributed to the difference in water content in the hydrated film as compared to the dry film. For regime II there are only small differences between the two film thicknesses, and in regime III as well the ellipsometric thickness is in good agreement with the QCM thickness. In regime IV there is a distinct deviation at a pH of 9 and pH 9.5, where the thickness of the dry film is larger. This variation might partly be due to the large uncertainty given by the scatter of the data. On the other hand, it has been observed in similar multilayer systems that adsorption under flow can cause lower adsorbed amounts as compared to adsorption by dipping into solutions without any flow.[23] This might be the reason why ellipsometric thickness here is larger than the thickness determined by QCM in the flow cell. In regime V the hydrated film thickness is slightly larger than that of the dry films.

Altogether, the results of modeling QCM data could be verified by the thickness measurements on dry films. The deviations of the thickness values are caused by hydration water, which leaves the film, when the PEM is dried for the ellipsometry measurements. This effect is most pronounced at the extreme pH values, i.e., region I and region V.

Determination of the Degree of Ionization of PAA by ATR-FTIR. To determine the degree of ionization of the PAA component, ATR-FTIR measurements of a PAA layer are performed. As a first layer PEI is adsorbed, and after a washing step a background spectrum is taken, before the PAA layer is adsorbed and measured. In Figure 7 the FTIR-ATR spectrum of the PAA layer deposited at a pH value of 4, and detected after washing, is shown.

In FTIR-ATR spectra of PAA the IR bands of the carbonyl group of the polyelectrolyte can be easily identified (see Figure 7). To determine the degree of ionization, the absorbance of the IR band of the symmetric vibration of the ionized carbonyl group at 1400 cm^{-1}, the absorbance of the asymmetric vibration of the ionized carbonyl group at 1552 cm^{-1}, and the absorbance of the C=O vibration at 1710 cm^{-1} were analyzed. The ratio of the ionized against all carbonyl resonances yields the degree of ionization according to the commonly applied expression[29]

$$\alpha = \frac{A_{vs}(COO^-) + A_{vas}(COO^-)}{(A_{vs}(COO^-) + A_{vas}(COO^-)) + 1.74A_v(C{=}O)} \quad (5)$$

The factor 1.74 has to be included in eq 5 to compensate for the different strength of the absorbance of the three IR bands.[29] The results of eq 5 for the pH values from 2 to 12 are shown in Figure 8.

At a pH of 2 the adsorbed PAA is nearly uncharged; the degree of ionization is less than 10%. With increasing pH value the degree of ionization increases rapidly, until at a pH value of 11 PAA is fully charged. The error of the data points is in the range of 10%. The pK_a value of PAA in the monolayer is determined as the pH value where $\alpha = 0.5$, which is found at pH = 4.5. This value is in good agreement with reported pK_a values of incorporated PAA in PEM, where it was found that the pK_a value of the PAA shifts by 1−4 pH units toward stronger acidity, depending on the layer number in the PEM.[21] Compared to the pK_a value of PAA in solution, where one finds a value of 6.5,[30] the pK_a is lower in layers, since the complexation with charges of opposite sign stabilizes the deprotonated form. Different values for the pK_a of PAA in solution have been reported by other authors, for example pK_a ∼5.7[31] and ∼5.8.[32] In any case, the pK_a value of PAA decreases due to the adsorption as a monolayer or in a multilayer assembly.

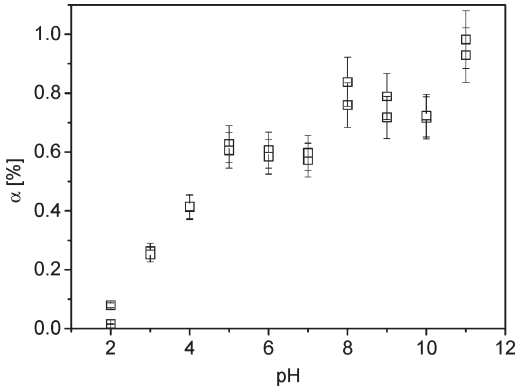

Figure 8. Degree of ionization of PAA in a monolayer in dependence on the pH value of deposition, as determined by ATR-FTIR.

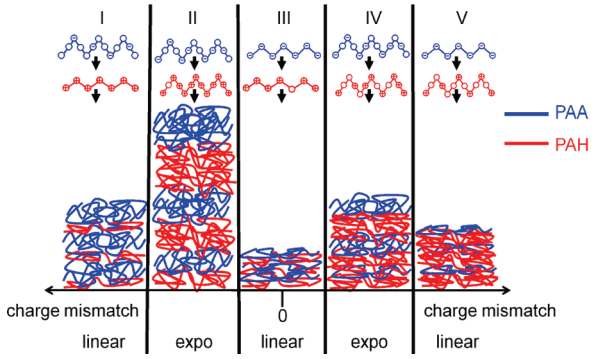

Figure 9. Growth behavior of PEM in dependence of charge mismatch, which is given as the difference of the absolute values of the linear charge density of PAA and PAH, respectively, indicating regions with different growth laws, exponential vs linear, and sketching the film composition.

Discussion

In this discussion we will compare the data from QCM-D, ellipsometry, and ATR-FTIR for each of the different pH regimes identified. We conclude on the mechanisms of layer formation for each regime separately and relate it to a dependence on the charge density on the chains. This will show that the pH dependence of layer formation is symmetric around region III and changes in the same manner toward higher and lower pH, since it is controlled by the charge dilution of the polycation or the polyanion, respectively.

Regime I. In the first regime from pH 3 to pH 4.5 the dissipation is high and comparatively thick films are formed. With increasing pH the frequency increment does not change much, while the dissipation strongly depends on pH (see Figure 1). The softness of the films in this regime can be explained by the large difference of the degree of ionization of the two polyelectrolytes: At pH 4.5 the weak acid PAA is only charged by about 50% (see Figure 8). On the other hand, the weak base PAH is nearly fully charged in regime I, since PAH has a pK_a value of 8−9 in solution.[30] In PEM the pK_a value of PAH is even larger, p$K_a \sim 10$;[21] thus, the PAH can be considered fully charged in this regime. The difference in the fraction of charged segments on either polyion can also be seen in the frequency change for each monolayer (see Figure 2): Most of the mass coverage increment originates from PAA, and only a small increment originates from PAH. This is consistent with findings for other polyelectrolyte pairs: when polyions of very different charge density are deposited alternatingly, the adsorbed mass is much higher for the polyion with lower charge density, yielding asymmetric layer buildup.[18,33] The reason is the fact that it is the charge per layer that has to match between subsequent layers in order to achieve optimized electrostatic complexation in the self-assembly process.

By increasing the pH value within regime I, and therefore charging PAA further, less PAA is needed to compensate the charges of PAH. In addition, the mass increment per PAH layer increases slightly (Figure 2) because PAH starts to discharge with increasing pH value; both changes cause a transition toward a more symmetric layer growth, since in this regime the charge densities along the chain become more similar to increasing pH value. This adjustment of the charge densities and the transition toward a more symmetric multilayer is also seen in the dissipation of the PEM, which decreases strongly with increasing pH value: The film becomes more rigid as the density of electrostatically complexed polycation and polyanion charges, which form cross-links between subsequent layers, increases. In this regime the growth law of the PEM is linear (see Figure 4). The thickness of the hydrated film at pH 3 is also larger than for the dry film. This indicates a large water content in the film at this pH value, which agrees well with the high dissipation, as it can be expected that soft PEM can take up more water.[34]

Regime II. In the second regime, which is in the pH region from pH 4.5 to pH 6, the frequency change is decreased massively and the PEM is less soft and very thick (see Figures 1 and 6). This increase is caused by large adsorbed amounts of both PAH and PAA (see Figure 2). The PAH and also the PAA adsorbed mass per layer reach a maximum in this region, and the layer buildup becomes more symmetric (see Figure 2). Figure 9 shows a sketch of the multilayer structure in dependence on pH. A large layer thickness for the pH values of regime II had already been reported for a dry layer pair of PAA and PAH by Shiratori.[18] Assuming a simple continuation of regime I, one would expect a further decrease of the PAA adsorbed amount since the charge density on the chain increases with pH and less material is required for charge compensation. However, the slight increase of Δf for PAA (see Figure 2) in combination with the sharp increase of Δf for PAH clearly marks the onset of a new growth mechanism.

This new growth mechanism is also clearly indicated by a sharp transition to exponential growth, which occurs at pH = 4.5 (see Figure 4). Exponential growth was originally found for a range of different strongly hydrated biopolymers with a comparatively low charge density,[14,35] as for example PGA/PAH.[13] Exponential growth was attributed to an interdiffusion of chains; i.e., chains from each newly adsorbed layer can diffuse into the PEM.[15] Thus, with each adsorption step more polymer is needed to overcompensate the charges of the previously deposited layer. It was accepted that biopolymers, due to −OH and free electron pairs of oxygen atoms causing a large hydration shell and low electrostatic binding forces, have sufficiently low interactions, such that interdiffusion is feasible. This is in contrast to simple linear chains with a much larger charge to weight ratio, where strong electrostatic interactions immobilize each adsorbed chain in the position of adsorption, causing linear growth. Here, in our present system, we observe an exponential growth of not highly hydrated chains, which is therefore opposed to the above principles: Regime II is characterized by a strong interaction between the polyions, since the charge-to-mass ratio is high, but yet a large mobility of adsorbed chains appears to be present as the polyions are apparently able to penetrate into the PEM. The strong interactions between PAA and PAH also become evident in the dissipation values in this regime, since it is only $\Delta D \approx 2$.

One might speculate how interdiffusion can occur in a film arrangement that involves strong electrostatic interaction,

while it does not play a role in regime I with much smaller electrostatic interaction. In regime II, the chains might be able to glide along each other and possibly penetrate into the film network by a reptation-type motion Therefore, in spite of the large thickness of about 150 nm (see Figures 5 and 6), the film is rigid at high frequencies, but not very compact, and the polyelectrolytes are still able to diffuse through the PEM. However, this changes when increasing the pH value further. Similar to the onset of regime II at lower pH, its termination is very sharply defined: At a pH value of 6 the interactions between the two polymers become too large for interdiffusion; it is seen that the mass increment decreases rapidly here, and simultaneously the exponentiality decreases (see Figure 4).

Regime III. In this regime from pH 6.5 to 7.5 the total adsorbed mass and the layer thickness have their lowest values. Here, both polyelectrolytes are nearly fully charged and behave like strong polyelectrolytes. Therefore, the formation of a rigid and flat film (see Figure 1) is expected and consistent with the general findings in the PEM literature.[36] In contrast to regime II, the polymers are not able to penetrate into the PEM, which can be attributed to a larger charge density of PAA, such that the interactions between the two polymers become too strong to allow interdiffusion. The dissipation is very low with a value of 1 or less, and both polyelectrolytes adsorb with an equal average mass increment per layer (see Figure 2). Thus, in this region the simple hit and stick model of polyelectrolyte adsorption holds. The thickness increment is only 0.75 nm per polymer layer and is therefore exactly in the range one expects for PEM buildup with strong polyelectrolytes and without salt in the polymer solution.[3,6] Here the PEM obeys a linear growth law (see Figure 4), typically observed for strong polyelectrolytes.

Regime IV. In this regime, ranging from pH 8 to pH 10, the frequency change increases again, but only to −200 to −300 Hz. The PEM also becomes softer with a dissipation value of 1.5 up to 3, and in this pH regime an exponential growth is found (see Figure 4). Altogether, the properties are very similar to those in regime II. Indeed, at a pH of 9 the difference between the charge densities of both polyelectrolyte chains is the same as in regime II, since in regime IV the pH value is higher than the pK_a value of PAH.[30] Here, PAA is nearly fully charged (see Figure 8), and PAH becomes less charged with increasing pH. Thus, the same situation as in regime II arises, only that here the charge density of PAA is high and that of PAH is low. Again, exponential growth, similarly strongly pronounced as in region II, is observed in a sharply defined pH region (see Figure 4), implying that the electrostatic interactions are again of an order allowing chain interdiffusion.

Thus, it does not seem to be relevant, which of the chains is charge diluted, and regimes II and IV are found symmetrically adjacent to regime III. This symmetry, however, is a qualitative finding and does not apply to the absolute values of the parameters. For example, mass coverage, dissipation, film thickness, and exponentiality do not have the same values as in regime II. Even further, the asymmetry shown in Figure 2 is inverted, as in both regimes PAH adsorption causes a larger mass increment in this regime as compared to PAA adsorption. This is probably due to the structural differences of the polycation and polyanion chains, which can lead to differences in the hydration behavior as well as in the mobility required for interdiffusion.

Regime V. In the last regime from pH 10 to 12 the frequency change decreases again from −200 to −80 Hz. The PEM becomes more rigid with a dissipation value of only 1 up to 1.5, and in this pH regime the growth again follows a linear law. The properties are qualitatively similar to those in regime I. Even the asymmetry of the multilayer is pronounced (Figure 2), only its dependence on pH differs from region I. In both regimes again asymmetric charge densities cause asymmetric multilayer formation. The total thickness decreases with increasing pH value, while it is constant in regime I. In spite of these few specific differences, however, the general picture is very similar in regimes I and V, and the symmetry between charge dilution of the polyacid or the polybase, respectively, is again clearly recognized.

Though several groups have already dealt with the pH dependence of layer-by-layer assembly of weak polyelectrolytes, even varying the solution pH of either polyelectrolyte solution separately,[16−18,25] nevertheless regimes with exponential layer growth laws have never been identified before. We think that this is attributed to the fact that some work was performed with intermediate washing steps at neutral pH, changing the dissociation of the chains during adsorption,[25] while other work was done on layer pairs.[17,18] In contrast to this, we ensured to keep the PEM at constant pH during the whole layer buildup, even employing pH-adjusted washing water and avoiding intermediate drying. As a control experiment, films prepared with intermediate washing steps at neutral pH show a very poor film quality and do not lead to reproducible results (data not shown). We believe that this cautious treatment is a key issue in obtaining layer formation properties and exponential growth regions that can be clearly attributed to the degree of charge of either chain.

Conclusions

We show here that in the alternating adsorption of a weak polyacid and a weak polybase interesting regimes with different growth laws and film properties can be found in dependence of the pH value during deposition. Qualitatively, the behavior is symmetric around an intermediate pH in the neutral region, where both polyions have a similar charge density, which is fairly large, about 50%. Here, they adsorb like strong polyelectrolytes in a flat geometry, forming thin layers with a linear growth law. Next to this regime, toward larger and lower pH, where one of the two polyion components becomes less charged, a regime of lower electrostatic interactions follows, where chains can penetrate into the layers, the consequence being exponential layer growth and very thick layers. At an even larger mismatch of charge density this interpenetration is disabled, and strongly asymmetric layer growth occurs with a linear growth law. Again, this tendency is symmetric and occurs in regimes I and V in a similar way. The most surprising finding certainly is the occurrence of sharply defined regimes of exponential layer growth, which had previously been mainly attributed to biopolymers.

Acknowledgment. The authors acknowledge financial support by the German Science Foundation ("Deutsche Forschungsgemeinschaft") within the research center SFB 458 "Ionic motion in disordered materials", which enabled the purchase of the ATR-FTIR equipment. We further thank Conny Cramer (WWU Münster) and Martin Müller (IPF Dresden) for helpful advice concerning the implementation of the ATR-FTIR technique.

References and Notes

(1) Decher, G.; Hong, J. D. *Makromol. Chem., Macromol. Symp.* **1991**, *46*, 321.
(2) Decher, G. *Photonic Optoelectron. Polym.* **1997**, *672*, 445.
(3) Dubas, S. T.; Schlenoff, J. B. *Macromolecules* **1999**, *32*, 8153.
(4) Decher, G.; Hong, J. D.; Schmitt, J. *Thin Solid Films* **1992**, *210*, 831.
(5) Büscher, K.; Graf, K.; Ahrens, H.; Helm, C. A. *Langmuir* **2002**, *18*, 3585.

(6) Lösche, M.; Schmitt, J.; Decher, G.; Bouwman, W. G.; Kjaer, K. *Macromolecules* **1998**, *31*, 8893.
(7) Tanchak, O. M.; Barrett, C. J. *Chem. Mater.* **2004**, *16*, 2734.
(8) Moya, S.; Donath, E.; Sukhorukov, G. B.; Auch, M.; Bäumler, H.; Lichtenfeld, H.; Möhwald, H. *Macromolecules* **2000**, *33*, 4538.
(9) Caruso, F.; Caruso, R. A.; Möhwald, H. *Science* **1998**, *282*, 1111.
(10) Schönhoff, M. *Curr. Opin. Colloid Interface Sci.* **2003**, *8*, 86.
(11) Decher, G.; Eckle, M.; Schmitt, J.; Struth, B. *Curr. Opin. Colloid Interface Sci.* **1998**, *3*, 32.
(12) Ramsden, J. J.; Lvov, Y. M.; Decher, G. *Thin Solid Films* **1995**, *254*, 246.
(13) Boulmedais, F.; Ball, V.; Schwinte, P.; Frisch, B.; Schaaf, P.; Voegel, J. C. *Langmuir* **2003**, *19*, 440.
(14) Picart, C.; Lavalle, P.; Hubert, P.; Cuisinier, F. J. G.; Decher, G.; Schaaf, P.; Voegel, J. C. *Langmuir* **2001**, *17*, 7414.
(15) Picart, C.; Mutterer, J.; Richert, L.; Luo, Y.; Prestwich, G. D.; Schaaf, P.; Voegel, J. C.; Lavalle, P. *Proc. Natl. Acad. Sci. U.S.A.* **2002**, *99*, 12531.
(16) Elzbieciak, M. K., M.; Zapotoczny, S.; Krastev, R.; Nowakoska, M.; Warszynski, P. *Colloids Surf.* **2009**, *343*, 89.
(17) Yoo, D.; Shiratori, S. S.; Rubner, M. F. *Macromolecules* **1998**, *31*, 4309.
(18) Shiratori, S. S.; Rubner, M. F. *Macromolecules* **2000**, *33*, 4213.
(19) Rmaile, H. H.; Schlenoff, J. B. *Langmuir* **2002**, *18*, 8263.
(20) Mendelsohn, J. D.; Barrett, C. J.; Chan, V. V.; Pal, A. J.; Mayes, A. M.; Rubner, M. F. *Langmuir* **2000**, *16*, 5017.
(21) Burke, S. E.; Barrett, C. J. *Langmuir* **2003**, *19*, 3297.
(22) Chung, A. J.; Rubner, M. F. *Langmuir* **2002**, *18*, 1176.
(23) Gauczinski, J.; Liu, Z.; Zhang, X.; Schönhoff, M. *Langmuir* **2010**, asap article, DOI: 10.1021/la1002447.
(24) Notley, S. M. E. M.; Wagberg, M. *J. Colloid. Interface Sci.* **2005**, *292*, 29.
(25) Fujii, N.; Fujimoto, K.; Michinobu, T.; Akada, M.; Hill, J. P.; Shiratori, S.; Ariga, K.; Shigehara, K. *Macromolecules* **2010**, Asap article, DOI: 10.1021/ma100473j.
(26) Sauerbrey, G. *Z. Phys.* **1959**, *155*, 206.
(27) Voinova, M. V.; Rodahl, M.; Jonson, M.; Kasemo., B. *Phys. Scr.* **1999**, *59*, 391.
(28) Schönhoff, M.; Ball, V.; Bausch, A. R.; Dejugnat, C.; Delorme, N.; Glinel, K.; Klitzing, R. V.; Steitz, R. *Colloids Surf., A* **2007**, *303*, 14.
(29) Müller, M.; Brissova, M.; Rieser, T.; Powers, A. C.; Lunkwitz, K. *Mater. Sci. Eng., C* **1999**, *8*−*9*, 163.
(30) Choi, J.; Rubner, M. F. *Macromolecules* **2005**, *38*, 116.
(31) Bromberg, L. *J. Phys. Chem. B* **1998**, *102*, 10736.
(32) Philippova, O. E.; Hourdet, D.; Audebert, R.; Khokhlov, A. R. *Macromolecules* **1997**, *30*, 8278.
(33) Rusu, M.; Kuckling, D.; Möhwald, H.; Schönhoff, M. *J. Colloid Interface Sci.* **2006**, *298*, 124.
(34) Tanchak, O. M.; Yager, K. G.; Fritzsche, H.; Harroun, T.; Katsaras, J.; Barrett, C. J. *Langmuir* **2006**, *22*, 5137.
(35) Lavalle, P. P.; Picart, C.; Cuisinier, F. J. G.; Decher, G.; Schaaf, P.; Voegel, J. C. *Biophys. J.* **2002**, *82*, 261.
(36) Schönhoff, M. *J. Phys.: Condens. Matter* **2003**, *15*, R1781.